Phys. Chem. Glasses, 2003, **44** (4), 296–302

Mixed doping in $Ge_{10}Se_{90-x-y}In_xBi_y$ glasses

N. Asha Bhat, K. S. Sangunni[1] *& A. Kumar*

Department of Physics, Indian Institute of Science, Bangalore-560 066, India

Manuscript received 12 June 2002
Revision received 6 January 2003
Accepted 22 January 2003

In this paper, we report our studies on indium–bismuth mixed doping in the $Ge_{10}Se_{90-x-y}In_xBi_y$ glassy system. Out of the four compositions studied in this glassy system, the contribution to the current for the compositions with x=*5 and* y=*10,* x=*10 and* y=*10 and* x=*5 and* y=*5 is mainly from electrons, while for the compositions with* x=*10 and* y=*5, it is mainly from holes. This* n- *and* p-*type conductivity and its origin in the mixed doped Ge–Se–In–Bi doped glasses are investigated using thermal, electrical and optical methods in order to understand the evolution of carrier type vis-a-vis the contributions from microscopic phase separation and defects.*

The focus of doping attempts in most chalcogenide glasses has so far been to obtain *n*-type conduction either from *p*-type or from intrinsic like characteristics. Unlike the situation in crystalline semiconductors, studies on mixed doped glassy semiconductors have been very rare, probably, the only instance being $(GeSe_{3\cdot5})_{88}Sb_{12-x}Bi_x$ system with Sb and Bi as the dopants.[1] The *p*-type conductivity in this system at $x = 0$ changes to *n*-type conductivity on adding nearly equal concentrations of Sb and Bi.

In chalcogenide glasses, earlier studies have shown that indium (In) from group III of the periodic table facilitates *p*-type conduction while bismuth (Bi) from group V facilitates *n*-type conduction.[2–6] If followed up, the mixed doping of In–Bi in chalcogenide glasses would have offered some insight into the mechanism driving evolution of carrier type. An ideal glassy system to study such mixed doping would be Se–In–Bi, having only one chalcogen element apart from indium and bismuth as dopants. Despite the poor glass forming tendency in this system, addition of Ge (which is known to enhance glass formation in Ge_xSe_{100-x} in the range $10 \leq x \leq 20$) offers the possibility of forming glassy semiconductors with simultaneous doping of In and Bi.[7] Four compositions in $Ge_{10}Se_{90-x-y}In_xBi_y$ with (x, y) taking values (5, 5), (5, 10), (10, 5) and (10, 10) are used to study the change of carrier type with mixed doping. Systematic studies carried out in the four compositions mentioned above yield some new results and shed light on the evolution of carrier type in chalcogenide glasses.

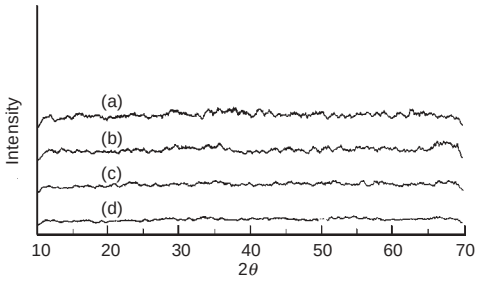

Figure 1. *X-ray diffraction patterns for glasses in $Ge_{10}Se_{90-x-y}In_xBi_y$ glasses: (a) $Ge_{10}Se_{80}In_5Bi_5$; (b) $Ge_{10}Se_{75}In_5Bi_{10}$; (c) $Ge_{10}Se_{75}In_{10}Bi_5$ and (d) $Ge_{10}Se_{70}In_{10}Bi_{10}$*

Experimental details

The four compositions in $Ge_{10}Se_{90-x-y}In_xBi_y$ system mentioned above were prepared using a conventional melt quenching technique. The samples prepared were subjected to x-ray diffraction (XRD) and differential scanning calorimetry (DSC) to confirm their amorphous and glassy nature. XRD studies were also carried out on the samples that crystallised. Subsequently, carrier type determination and temperature dependent resistivity measurements were obtained using an experimental set-up designed for the purpose.[8] For optical band gap determination, glassy samples in powdered form were subjected to optical absorption studies using a Hitachi U-3410 spectrophotometer with a scan rate of 120 nm/min. Prior to the scans on each sample, the spectrometer was calibrated in the wavelength region of interest for base line correction. Photoluminescence spectroscopic investigations were also carried out to study the role played by defects on carrier type evolution using a Midac Fourier transform photoluminescence spectrometer.

Results

Structural and thermal studies

Figure 1 depicts the XRD patterns for the four as-prepared samples in $Ge_{10}Se_{90-x-y}In_xBi_y$ system. It is evident that all the compositions of interest are x-ray

[1] Author to whom correspondence should be addressed. (email: sangu@physics.iisc.ernet.in)

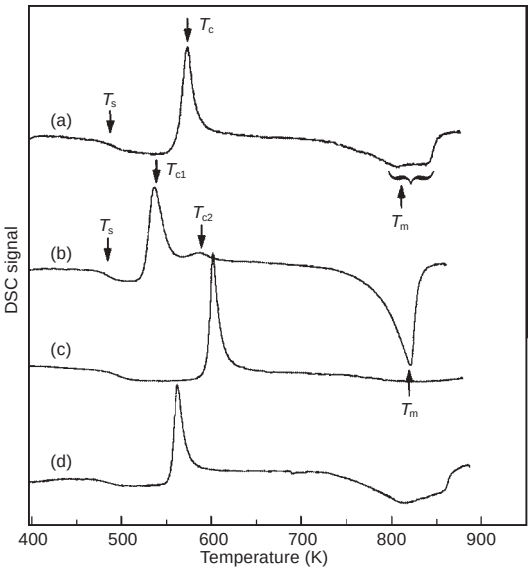

Figure 2. *DSC scans with 20 K/min rate for glasses in $Ge_{10}Se_{90-x-y}In_xBi_y$ glasses: (a) $Ge_{10}Se_{80}In_5Bi_5$; (b) $Ge_{10}Se_{75}In_5Bi_{10}$; (c) $Ge_{10}Se_{75}In_{10}Bi_5$ and (d) $Ge_{10}Se_{70}In_{10}Bi_{10}$*

amorphous. The subsequent thermal characterisation carried out using DSC with a heating rate of 20 K/min is given in Figure 2. It can be seen from the figure that all compositions undergo a glass transition followed by crystallisation. While each of the three compositions, namely, $Ge_{10}Se_{80}In_5Bi_5$, $Ge_{10}Se_{75}In_{10}Bi_5$ and $Ge_{10}Se_{70}$ $In_{10}Bi_{10}$ exhibit a single crystallisation exotherm, the composition $Ge_{10}Se_{75}In_5Bi_{10}$ exhibits two crystallisation exotherms. In addition, broad melting transitions follow the single exotherms in $Ge_{10}Se_{80}In_5Bi_5$ and $Ge_{10}Se_{70}In_{10}Bi_{10}$, and a single melting transition follows the two exotherms in $Ge_{10}Se_{75}In_5Bi_{10}$. No melting transition was observed for $Ge_{10}Se_{75}In_{10}Bi_5$ composition below 873 K.

X-ray diffraction patterns of the crystallised phases corresponding to each DSC exotherm of the four compositions are shown in Figures 3–5. A careful analysis of these patterns using standard procedures reveals that the single DSC exotherm observed for $Ge_{10}Se_{80}In_5Bi_5$ corresponds to a combined crystallisation of two phases β-In_2Se_3 and rhombohedral Bi_2Se_3, Figure 3.[9,10] However, the single DSC exotherm of $Ge_{10}Se_{70}In_{10}Bi_{10}$ corresponds to the crystallisation of only β-In_2Se_3,

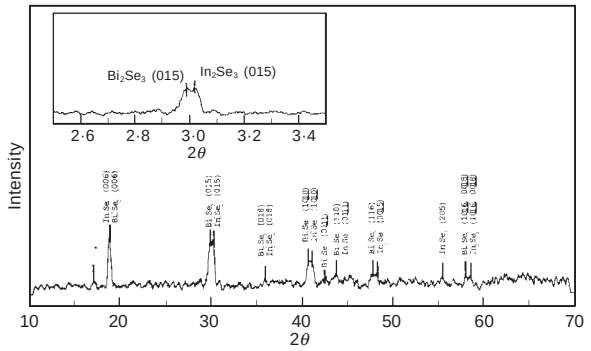

Figure 3. *XRD pattern for crystallised $Ge_{10}Se_{80}In_5Bi_5$ glass at 2 °/min scan rate. The peak positions that could not be identified with any known reflection are marked by (*). The two peaks around 2θ=30° are clearly seen under the expanded scale shown in the inset*

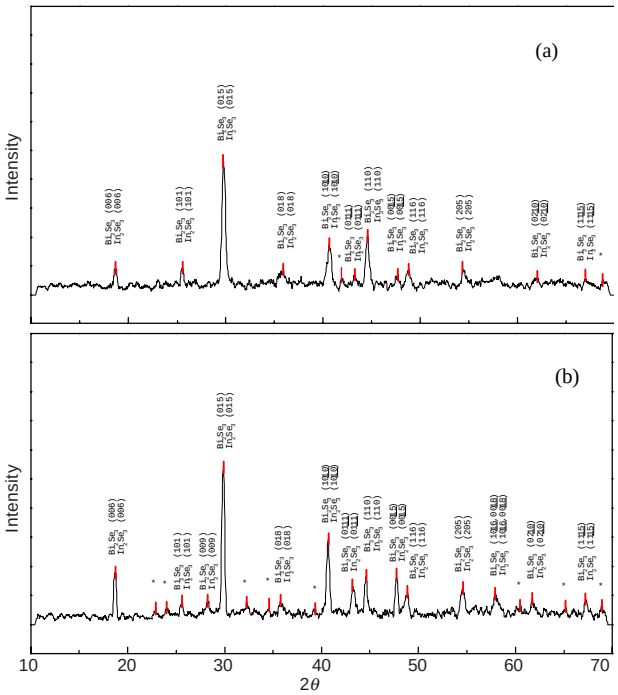

Figure 4. *XRD patterns with 2 °/min scan rate for $Ge_{10}Se_{75}In_5Bi_{10}$ glass crystallised at (a) T_{c1} and (b) T_{c2}. The peak positions that could not be identified with any known reflection are marked by* (*)

Figure 5(b). Interestingly, though there are two DSC exotherms for $Ge_{10}Se_{75}In_5Bi_{10}$, there is near matching between the corresponding twin XRD patterns, Figure 4, with a few 'd' values becoming more pronounced in the pattern corresponding to the second exotherm. Moreover, most of the 'd' values in the twin XRD patterns nearly match the average 'd' values of β-In_2Se_3

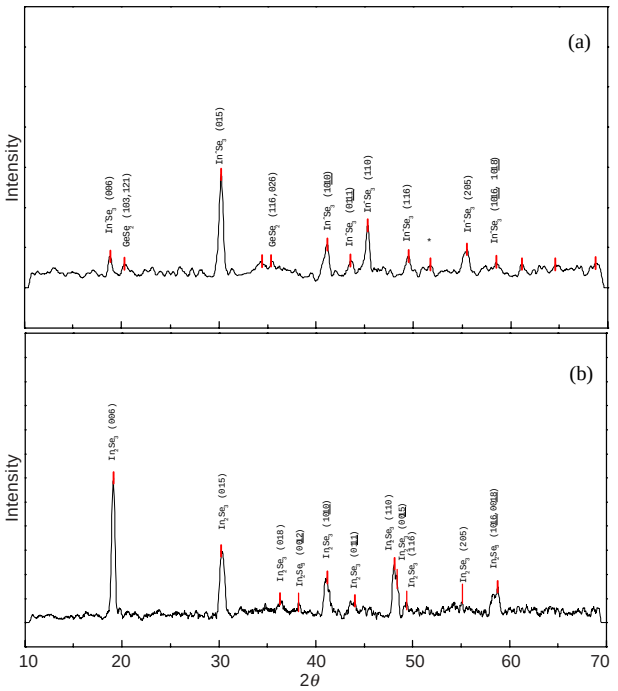

Figure 5. *XRD patterns with 2 °/min scan rate for (a) $Ge_{10}Se_{75}In_{10}Bi_5$ and (b) $Ge_{10}Se_{70}In_{10}Bi_{10}$ glasses crystallised at their respective crystallisation temperatures. The peak positions that could not be identified with any known reflection are marked by* (*)

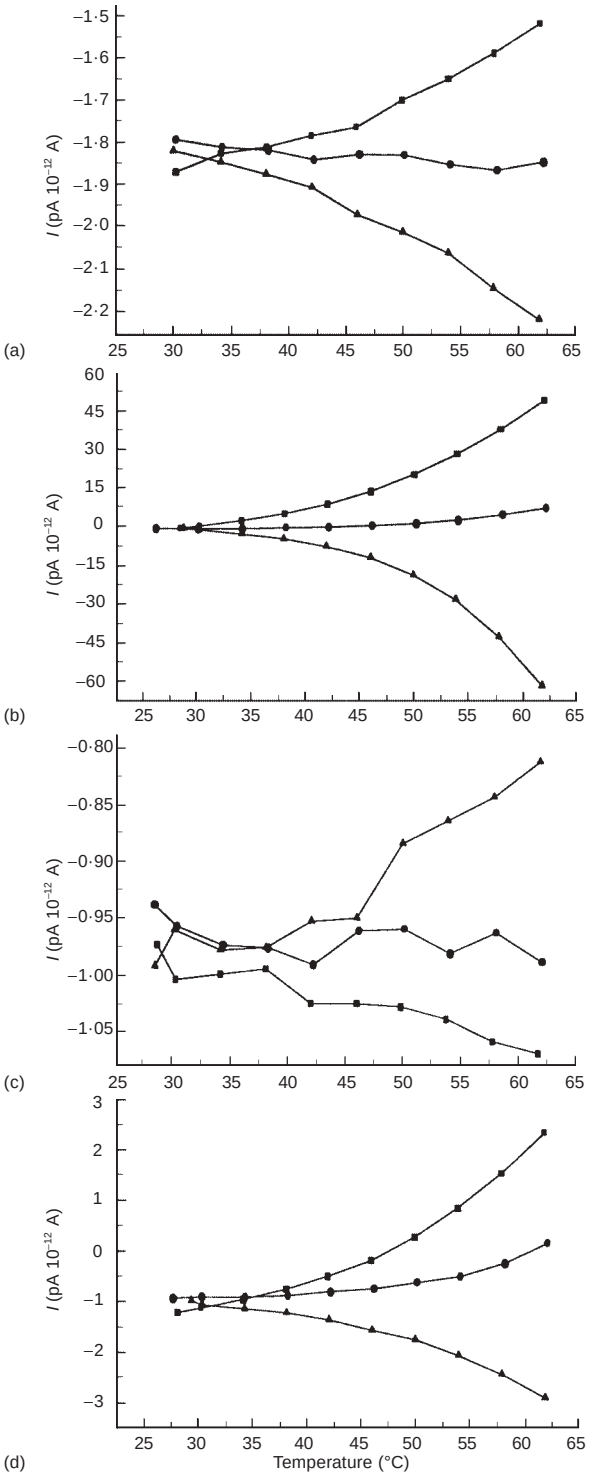

Figure 6. *Variations in carrier currents with positive, negative and zero temperature gradients for (a) $Ge_{10}Se_{80}In_5Bi_5$; (b) $Ge_{10}Se_{75}In_5Bi_{10}$; (c) $Ge_{10}Se_{75}In_{10}Bi_5$ and (d) $Ge_{10}Se_{70}In_{10}Bi_{10}$ glasses*
▲ ΔT, +ve ■ ΔT, –ve ◆ ΔT, ~0

and rhombohedral Bi_2Se_3. Based on this trend and the comparison of relative intensities of XRD peaks, there appears to be a single rhombohedral-like (or Bi_2Se_3) structure evolving in two stages with uniform distribution of indium and bismuth in most of its (hkl) planes. The single melting transition observed especially for this composition supports such a possibility.

Table 1. *Different experimental parameters observed for $Ge_{10}Se_{90-x-y}In_xBi_y$ glasses*

Sample	*Carrier type*	I *(pA)*	E_s *(eV)*	E_g *(eV)*	*(D^+/D^-) (Table 2)*
$Ge_{10}Se_{80}In_5Bi_5$	n	0·3	0·691	1·404	1·988
$Ge_{10}Se_{75}In_5Bi_{10}$	n	60	0·572	1·438	1·438
$Ge_{10}Se_{75}In_{10}Bi_5$	p	~0·15	0·660	1·483	–
$Ge_{10}Se_{70}In_{10}Bi_{10}$	n	2	0·661	1·572	–

For the fourth $Ge_{10}Se_{75}In_{10}Bi_5$ composition, the XRD pattern corresponding to the single DSC exotherm can be better indexed with a combination of 'd' values corresponding to β-In_2Se_3 and orthorhombic $GeSe_2$, Figure 5(a).[11] Such crystallised phases probably melt at temperatures beyond 873 K. The overall trend indicates that all four compositions crystallise only partially leaving behind a background amorphous or glassy matrix.

Carrier type determination and resistivity measurements

The variations of carrier current at different temperatures for positive, negative and zero temperature gradients (ΔT) for all four compositions of interest are presented in Figure 6(a)–6(d). From these figures, it is evident that the current flow in $Ge_{10}Se_{80}In_5Bi_5$, $Ge_{10}Se_{75}In_5Bi_{10}$ and $Ge_{10}Se_{70}In_{10}Bi_{10}$ varies in the negative (positive) direction when the temperature gradient changes in the positive (negative) direction. However for the fourth composition $Ge_{10}Se_{75}In_{10}Bi_5$, the direction of the current flow, evident only above 45°C (ΔT~10 °C), is along the direction in which the temperature gradient varies. To get an idea on how the carrier current evolves with In–Bi mixed doping, the magnitude of carrier currents for all four compositions at a temperature gradient of nearly 30°C are tabulated in Table 1.

Figure 7(a) and (b) shows the logarithmic variations in temperature dependent normalised resistivity (ρ_T/ρ_{RT}) for the four compositions. The values of activation energy for electrical conductivity E_σ determined from the slopes of $\ln(\rho_T/\rho_{RT})$ versus $1/T$ plots are tabulated in Table 1. It is interesting to note that the value of E_σ, also known as the electrical band gap, is significantly lower for $Ge_{10}Se_{75}In_5Bi_{10}$ as compared to that for the other compositions.

Optical absorption and photoluminescence

In chalcogenide glasses the dependence of absorption coefficient (α) on energy (E) in a region of the absorption spectrum where a strong absorption sets in can be written as[12]

$$\alpha = \alpha_0 \frac{\left(E - E_g\right)^2}{E}$$

where α_0 represents the pre-exponential factor and E_g is the optical band gap. For powdered samples with percentage absorbance given by A, the above formula can be rewritten as

$$A = C \frac{\left(E - E_g\right)^2}{E}$$

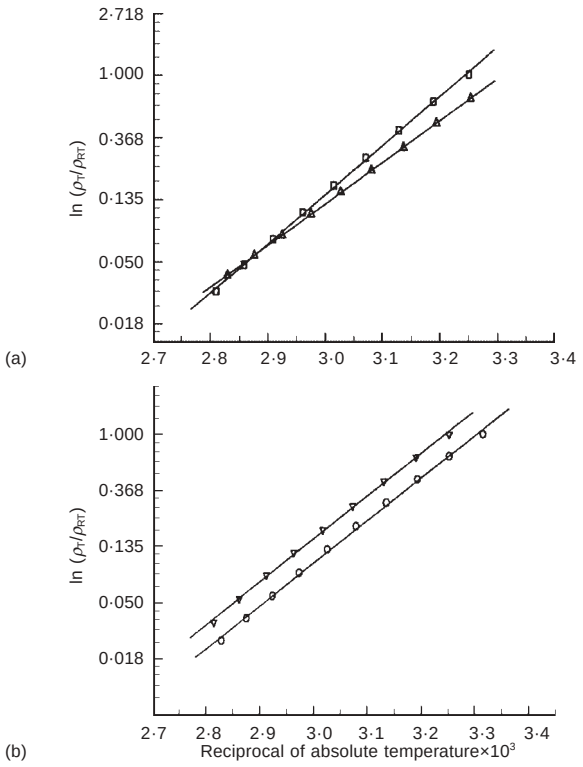

Figure 7. *Plots of ln(ρT/ρRT) versus 1000/T(K) for the fourcompositions of interest in $Ge_{10}Se_{90-x-y}In_xBi_y$ system. The linear fits to the experimental data are also shown*
—— linear fit
(a) experimental, □ $Ge_{10}Se_{80}In_5Bi_5$ △ $Ge_{10}Se_{75}In_5Bi_{10}$
(b) experimental, ○ $Ge_{10}Se_{750}In_{10}Bi_5$ ▽ $Ge_{10}Se_{70}In_{10}Bi_{10}$

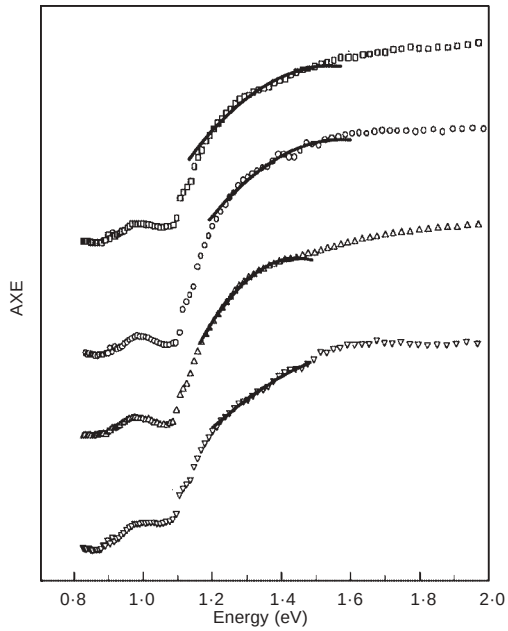

Figure 8. *Variation of the product (*AE*) versus* E *for different glass compositions in $Ge_{10}Se_{90-x-y}In_xBi_y$. A second order polynomial fitted in the region III of the absorption spectrum is also shown*
□ $Ge_{10}Se_{80}In_5Bi_5$ △ $Ge_{10}Se_{75}In_{10}Bi_5$
○ $Ge_{10}Se_{75}In_5Bi`_{10}$ ▽ $Ge_{10}Se_{70}In_{10}Bi_{10}$
— polynomial fit

where C is a constant dependent on the relationship between α and A. Rewriting again

$$AE=CE^2+CE_g^2-2CE_gE$$

The product (AE), calculated from the experimental data on absorbance (A) at different energies (E), is plotted versus E for all four compositions in Figure 8. As shown in the figure, the absorption spectra in strong absorption region was fitted to a second order polynomial function in E. The band gap values (E_g) for all four compositions are calculated using the best fit values obtained for C, CE_g^2 and $2CE_g$ and are given in Table 1.

It has been found that only two out of the four compositions, namely $Ge_{10}Se_{80}In_5Bi_5$ and $Ge_{10}Se_{75}In_5Bi_{10}$ exhibit luminescence at 4·2 K with Ar^+ laser excitation (λ=514·5 nm). The PL spectra recorded for these two compositions are shown in Figures 9(a) and 9(b). The luminescence spectra of these compositions show fine features indicating radiative transition at three different energies, in line with the features observed for a-Se and Bi-doped Ge–Se and Ge–Se–Te glasses.[13] The best fit parameters for the three transitions, determined by deconvoluting the experimental spectra using LM algorithm, are given in Table 2.

Discussion

The crystallisation exotherms observed for all four compositions indicate that In–Bi doped glasses phase separate at macroscopic levels on heating. In general, such macroscopic phase separation in multicomponent glasses is a pointer to the presence of relevant structural units at microscopic level. From the XRD patterns for crystallised glasses, the possible structural units that contribute to the crystallisation of $Ge_{10}Se_{80}In_5Bi_5$ and $Ge_{10}Se_{75}In_5Bi_{10}$ compositions are $InSe_{3/2}$ and $BiSe_{3/2}$. If these structural units are distributed homogeneously in the glassy matrix, they may crystallise into different phases at the same crystallisation temperature in $Ge_{10}Se_{80}In_5Bi_5$, like the homogeneously distributed $GeSe_{4/2}$ and $Se_{2/2}$ structural units crystallise into $GeSe_2$ and tetragonal Se at a single temperature in Ref. 14. On the other hand, if the structural units are distributed inhomogeneously in the host glassy matrix and are to evolve into a single crystalline phase, the transition may involve two stages as observed in $Ge_{10}Se_{75}$ In_5Bi_{10}. Likewise, the crystallisation of a single phase, β-In_2Se_3, in $Ge_{10}Se_{70}In_{10}Bi_{10}$ in a single stage can also be explained. As the composition has both indium and bismuth at 10 at%, one can expect both $InSe_{3/2}$ and $BiSe_{3/2}$ structural units to be present with equal probability. Notwithstanding this fact, the composition crystallises into only β-In_2Se_3 phase probably due to the fact that the distribution of $InSe_{3/2}$ facilitates its participation in crystallisation, while the distribution of $BiSe_{3/2}$ structural units does not. This can be due to a large mismatch in the distribution of regions containing $InSe_{3/2}$ and $BiSe_{3/2}$ structural units.

On the other hand, for $Ge_{10}Se_{80}In_{10}Bi_5$ glass, the crystallisation of both β-In_2Se_3 and orthorhombic $GeSe_2$ at the same temperature could be an indication for the corresponding structural units being distributed homogeneously. However, the regions containing

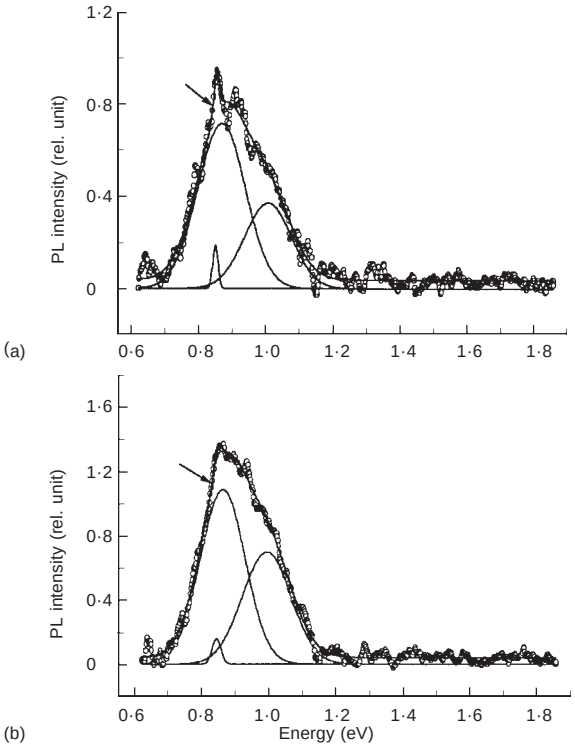

Figure 9. *Experimental PL spectra for (a) $Ge_{10}Se_{80}In_5Bi_5$ and (b) $Ge_{10}Se_{75}In_5Bi_{10}$ glasses at 4·2 K and 150 mWcm^{-2} incident power density. The experimental spectra were deconvoluted into three Gaussian distributions (1–3) each and the resultants (4) of these matches well with the experimental spectra*
○ experimental —— deconvoluted

$BiSe_{3/2}$ structural units in this composition also do not facilitate Bi_2Se_3 crystallisation, like in $Ge_{10}Se_{70}In_{10}Bi_{10}$. These observations suggest that addition of Bi facilitates in the inhomogeneous distribution of structural units in the glassy matrix of $Ge_{10}Se_{90-x-y}In_xBi_y$. The most likely consequence of such a distribution of structural units is the setting in of structural inhomogeneities at microscopic level or microscopic phase separation in the host glassy matrix.

The temperature dependent trends in carrier currents suggest that the contribution to current in $Ge_{10}Se_{80}In_5Bi_5$, $Ge_{10}Se_{75}In_5Bi_{10}$ and $Ge_{10}Se_{70}In_{10}Bi_{10}$ comes largely from electrons whereas for $Ge_{10}Se_{75}In_{10}Bi_5$ it comes largely from holes.[15] A comparison of carrier currents at a fixed temperature gradient for different compositions in Table 1 suggests that the carrier current for $Ge_{10}Se_{75}In_5Bi_{10}$ is significantly higher compared to that for the other three compositions. Also, the two orders of magnitude jump in carrier current for $Ge_{10}Se_{75}In_5Bi_{10}$, brought out by the addition of 5 at% of Bi to $Ge_{10}Se_{80}In_5Bi_5$, reduces by an order of magnitude for $Ge_{10}Se_{70}In_{10}Bi_{10}$. On the other hand, the near *p*-type characteristic of $Ge_{10}Se_{75}In_{10}Bi_5$ suggest that addition of 5 at% of In to $Ge_{10}Se_{80}In_5Bi_5$ brings out a change in the contribution characteristics of the carrier current. The trends suggest that addition of indium and bismuth have opposite roles to play in deciding the carrier type in $Ge_{10}Se_{90-x-y}In_xBi_y$ glasses. This is also evident from the compositional variation in the activation energy for electrical conduction (E_σ). The value of $\boldsymbol{E}_\sigma$ with the addition of 5 at% Bi to $Ge_{10}Se_{80}In_5Bi_5$, i.e. $Ge_{10}Se_{75}In_5Bi_{10}$, gets nearly compensated for $Ge_{10}Se_{70}\ In_{10}Bi_{10}$. An overall indication of these observations is that Bi addition in chalcogenide glasses improves *n*-type conduction while In addition facilitates *p*-type conduction. In other words, in chalcogenide glasses, Bi acts as an effective donor and In acts as an effective acceptor, even under mixed doped conditions.

A comparison of the optical band gap (E_g), activation energy for electrical conduction (E_σ) and the evolution in carrier type with In–Bi mixed doping suggests the following trends.

1. The Fermi level E_F is nearly pinned at the middle of the band gap for $Ge_{10}Se_{80}In_5Bi_5$.
2. For $Ge_{10}Se_{75}In_5Bi_{10}$ and $Ge_{10}Se_{70}In_{10}Bi_{10}$, the position of E_F is nearer to the conduction band mobility edge than to the valence band mobility edge.
3. For $Ge_{10}Se_{75}In_{10}Bi_5$, position of E_F is relatively closer to the valence band mobility edge.

The above observations on the position of the Fermi level E_F, when combined with the observations on carrier type evolution, pose three questions: (i) How does the composition $Ge_{10}Se_{80}In_5Bi_5$ with its Fermi level almost pinned exhibit *n*-type characteristics? (ii) Why is the carrier current in $Ge_{10}Se_{75}In_{10}Bi_5$ marginally lower despite its Fermi level being significantly closer to the valance band mobility edge? (iii) Why is the carrier current for $Ge_{10}Se_{70}In_{10}Bi_{10}$ an order of magnitude less compared to that for $Ge_{10}Se_{75}In_5Bi_{10}$, in spite of the fact that both the compositions have the same concentration of Bi, i.e. 10 at%?

In a semiconductor, both electrons and holes can contribute to current simultaneously. If carriers of both types are present in almost equal numbers but with different drift mobilities, then the effective contribution to the current comes from the carriers that have a greater drift mobility.[16,17] As an example, the possibility of drift mobility of electrons being effectively greater than that of holes will result in an effective contribution to the current from electrons rather than from holes even in a case where the Fermi level is pinned.[17] Based on these facts, the *n*-type characteristic shown by of $Ge_{10}Se_{80}In_5Bi_5$, having a pinned Fermi level, can be attributed to the greater mobility of electrons. Similarly, for $Ge_{10}Se_{75}In_{10}Bi_5$, the position of E_F being closer to the valence band mobility edge implies the presence of more numbers of holes than electrons. In spite of this fact, if the drift mobility of electrons is greater than that of holes, the effective contribution of holes to the

Table 2. *Parameters extracted from deconvoluting the experimental PL spectra including the area (in relative units)*

Sample	xc_1 *(eV)*	*FWHM (eV)*	*Area*	xc_2 *(eV)*	*FWHM (eV)*	*Area*	xc_3 *(eV)*	*FWHM (eV)*	*Area*
$Ge_{10}Se_{80}In_5Bi_5$	0·850	0·019	0·037	0·866	0·168	1·276	1·01	0·163	0·642
$Ge_{10}Se_{75}In_5Bi_{10}$	0·845	0·031	0·053	0·862	0·158	1·831	0·993	0·171	1·273

current can reduce significantly. This explains considerably low hole current observed for $Ge_{10}Se_{75}In_{10}Bi_5$. To answer the third question, one can note that the energy separation between E_F and the conduction band mobility edge for the composition $Ge_{10}Se_{70}In_{10}Bi_{10}$ exceeds that for $Ge_{10}Se_{75}In_5Bi_{10}$ by nearly 0·1 eV. The significantly lower carrier current for a fixed temperature gradient in the former composition as compared to that in the latter will then be a natural consequence.

In chalcogenide glasses, the contribution to photoluminescence is mainly due to the radiative recombinations occurring at inherent D^+ (or C_3^+) and D^- (or C_1^-) defects.[18] These inherent defects can be either randomly distributed to form valence alternation pairs or nonrandomly distributed to form *intimate* valence alternation pairs (IVAPs).[19] Following the arguments presented for the deconvoluted spectra for Bi doped Ge–Se and Ge–Se–Te glasses elsewhere, the deconvoluted spectra in the present case can also be identified with different transitions involving defect levels.[13] As in Bi doped Ge–Se and Ge–Se–Te glasses, the narrow deconvoluted spectrum can be identified with the radiative transition occurring at nonrandom D^+ and D^-. Likewise, the two broader deconvoluted spectra can be identified with radiative transitions occurring at random D^+ and D^-, the one at lower energy being due to the transitions occurring at random D^+ defects. This scheme of identification of the deconvoluted spectra with radiative transition at specific defects reveals a reduction in the relative concentration of D^+ defects as compared to D^- defects with Bi addition.

Absence of PL for the two samples having 10 at% of indium can be due to the contribution of some nonradiative routes.[18] A unique nonradiative route considered especially for chalcogenide glasses namely the creation of light induced metastable nonradiative centres can also play a significant role in obscuring luminescence.[19] However, the present investigations clearly suggest that above a certain level, addition of indium brings down luminescence efficiency in chalcogenide glasses.

Mixed doping: role of phase separation and defects

Addition of Bi in $Ge_{10}Se_{90-x-y}In_xBi_y$ mixed doped system facilitates nonuniform distribution of $BiSe_{3/2}$ and $InSe_{3/2}$ structural units and renders the glassy matrix structurally inhomogeneous or phase separated at a microscopic level. To some extent, the evidences are similar to that occurring in Bi doped $Ge_{20}Se_{80-x}Bi_x$ and $Ge_{20}Se_{70-x}Te_{10}Bi_x$ glasses. As a result, like in these two glassy systems, the setting in of inhomogeneous characteristics in mixed-doped $Ge_{10}Se_{90-x-y}In_xBi_y$ can also be traced to *a*-Bi_2Se_3 phase separation at microscopic level rather than to *c*-Bi_2Se_3 phase separation.[20] For structurally inhomogeneous glassy matrices with improved connectivity for electrical transport, the current can enhance significantly as in $Ge_{10}Se_{75}In_5Bi_{10}$. In addition, an order of magnitude higher carrier current for microscopically inhomogeneous $Ge_{10}Se_{70}In_{10}Bi_{10}$ as compared to that for the more homogeneous $Ge_{10}Se_{80}In_5Bi_5$ confirms yet again the role played by structural inhomogeneities in improving *n*-type conduction. The significantly low carrier currents for the more homogeneous $Ge_{10}Se_{80}In_5Bi_5$ and $Ge_{10}Se_{75}In_{10}Bi_5$ compositions substantiate the fact that homogeneous microscopic structures in glassy matrices reduce the connectivity for electrical transport.

As in the case of the two glassy systems studied earlier, the imbalance observed in the concentrations of D^+ and D^- defects for $Ge_{10}Se_{75}In_5Bi_{10}$ glass, Table 1, can contribute extra electrons and reduce the effective drift mobility of holes. The improved *n*-type conduction observed for this composition thus substantiates the role played by inherent defects in facilitating *n*-type conduction.

Conclusions

When indium (In) and bismuth (Bi) are doped simultaneously in the $Ge_{10}Se_{90-x-y}In_xBi_y$ glassy system, the compositions with x=5 and y=10; x=10 and y=10 and x=5 and y=5 show *n*-type conduction revealing the greater contribution of electrons to the carrier current. For the composition with x=10 and y=5, the contribution to current is mainly from holes. For x=5, y=10, the glass crystallises into a single phase in two stages whereas for x=10, y=10, the glass crystallises into a single phase in one stage. On the other hand, each of the other two compositions crystallises into two phases in a single stage. For x=5, y=10 and x=10, y=10, the regions containing $BiSe_{3/2}$ and $InSe_{3/2}$ structural units are inhomogeneously distributed. For the other two compositions, these regions are homogeneously distributed in the host glassy matrix. The contribution of electrons to current in x=5, y=10 far exceeds the same in the other two *n*-type conducting compositions. The presence of structural inhomogeneities at microscopic level is one of the reasons for such a large current. Photoluminescence studies suggest that reduction in relative concentration of D^+ defects favours a greater contribution of electrons to the current. In essence, the contribution of indium to electrical transport is opposite to that of Bi.

In summary, the glassy system $Ge_{10}Se_{90-x-y}In_xBi_y$ provides a scope to study the effects of incorporating additional elements in *n*-type conducting Bi doped samples. The studies show that indium (In) addition induces a reversal of electrical and structural changes brought out by bismuth (Bi) addition. When the contribution of extra electrons accompanies the setting in of structural inhomogeneities, the current in the corresponding glassy matrix enhances significantly like in $Ge_{10}Se_{75}In_5Bi_{10}$. The present studies also reveal that improved *n*-type conduction with Bi addition is associated with a significant shift in Fermi level towards the conduction band. This is augmented by inhomogeneities at microscopic level and a substantial reduction in the relative concentration of D^+ defects.

References

1. Nagels, P., Tichy, L., Triska, A. & Ticha, H. J. *Non-Cryst. Solids*, 1983, **59&60**, 1015.
2. Kumar, A., Manzar, M. M., Zulfequar, M., Kumar, A. & Husain, M. *Solid State Commun.*, 1991, **79**, 699.
3. Tohge, N., Yamamoto, Y., Minami, T. & Tanaka, M. *Appl. Phys. Lett.*, 1979, **34**, 640.

4. Tohge, N., Minami, T. & Tanaka, M. *J. Non-Cryst. Solids*, 1980, **37**, 23.
5. Nagels, P., Tichy, L., Triska, A. & Ticha, H. *J. Non-Cryst. Solids*, 1983, **59&60**, 1015.
6. Bhatia, K. L., Parthasarathy, G., Sharma, A. & Gopal, E. S. R. *Phys. Rev. B*, 1988, **38**, 6342.
7. Phillips, J. C. *Physics Today*, February 1982, 27.
8. Asha Bhat, N. & Sangunni, K. S. *J. Instrum. Soc. India*, 2000, **30**, 29.
9. *Powder Diffraction File*. Set.35-1056. (for β-In_2Se_3).
10. *Powder diffraction File*. Set. 33-214. (for Bi_2Se_3).
11. *Powder Diffraction File*. Set. 32-410. (for orthorhombic $GeSe_2$).
12. Connell, G. A.N. In *Topics in applied physics: amorphous semiconductors*.Vol. 36. 1979. Edited by M. H. Brodsky. Springer-Verlag, Berlin. P 73.
13. Asha Bhat, N., Sangunni, K. S. & Rao, K. S. R. K. *J. Optoelectron. Adv. Mater.*, 2001, **3**, 735.
14. Rabinal, M. K. *PhD Thesis*. Indian Institute of Science, Bangalore. 1993.
15. Damodar Das, V. *Introduction to thermoelectric effects: methods of thermoelectric characterization of materials*. 1993. Aparna Publishers, Mysore, India.
16. Takahashi, T. *J. Non-Cryst. Solids*, 1981, **44**, 239.
17. Streetman,B. G. *Solid state electronics devices*. 1995, Prentice-Hall, New Delhi, India.
18. Street, R. A. *Adv. Phys.*, 1976, **25**, 397 and references therein.
19. Davis, E. A. In *Topics in applied physics: amorphous semiconductors*. Vol. 36. 1979. Edited by M. H. Brodsky. Springer-Verlag, Berlin. P 41.
20. AshaBhat, N. & Sangunni, K. S. *Solid State Commun.*, 2000, **116**, 297.